25. Degtyarev M, De Maziere A, Orr C, Lin J, Lee BB, Tien JY, et al. Akt inhibition promotes autophagy and sensitizes PTEN-null tumors to lysosomotropic agents. J Cell Biol 2008; 183:101-16.
26. Wan X, Harkavy B, Shen N, Grohar P, Helman LJ. Rapamycin induces feedback activation of Akt signaling through an IGF-1R-dependent mechanism. Oncogene 2007; 26:1932-40.
27. Sun SY, Rosenberg LM, Wang X, Zhou Z, Yue P, Fu H, Khuri FR. Activation of Akt and eIF4E survival pathways by rapamycin-mediated mammalian target of rapamycin inhibition. Cancer Res 2005; 65:7052-8.
28. O'Reilly KE, Rojo F, She QB, Solit D, Mills GB, Smith D, et al. mTOR inhibition induces upstream receptor tyrosine kinase signaling and activates Akt. Cancer Res 2006; 66:1500-8.
29. Cirstea D, Hideshima T, Rodig S, Santo L, Pozzi S, Vallet S, et al. Dual inhibition of akt/mammalian target of rapamycin pathway by nanoparticle albumin-bound-rapamycin and perifosine induces antitumor activity in multiple myeloma. Mol Cancer Ther 2010; 9:963-75.
30. Aoki H, Takada Y, Kondo S, Sawaya R, Aggarwal BB, Kondo Y. Evidence that curcumin suppresses the growth of malignant gliomas in vitro and in vivo through induction of autophagy: role of Akt and extracellular signal-regulated kinase signaling pathways. Mol Pharmacol 2007; 72:29-39.
31. Ellington AA, Berhow MA, Singletary KW. Inhibition of Akt signaling and enhanced ERK1/2 activity are involved in induction of macroautophagy by triterpenoid B-group soyasaponins in colon cancer cells. Carcinogenesis 2006; 27:298-306.
32. Rubinsztein DC, Gestwicki JE, Murphy LO, Klionsky DJ. Potential therapeutic applications of autophagy. Nat Rev Drug Discov 2007; 6:304-12.
33. Ravikumar B, Vacher C, Berger Z, Davies JE, Luo S, Oroz LG, et al. Inhibition of mTOR induces autophagy and reduces toxicity of polyglutamine expansions in fly and mouse models of Huntington disease. Nat Genet 2004; 36:585-95.
34. Kotake Y, Ohta S. MPP$^+$ analogs acting on mitochondria and inducing neuro-degeneration. Curr Med Chem 2003; 10:2507-16.
35. Hagan MP, Hopcia KL, Sylvester FC, Held KD. Caffeine-induced apoptosis reveals a persistent lesion after treatment with bromodeoxyuridine and ultraviolet-B light. Radiat Res 1997; 147:674-9.
36. Efferth T, Fabry U, Glatte P, Osieka R. Expression of apoptosis-related oncoproteins and modulation of apoptosis by caffeine in human leukemic cells. J Cancer Res Clin Oncol 1995; 121:648-56.
37. Shinomiya N, Takemura T, Iwamoto K, Rokutanda M. Caffeine induces S-phase apoptosis in cis-diamminedichloroplatinum-treated cells, whereas cis-diamminedichloroplatinum induces a block in G_2/M. Cytometry 1997; 27:365-73.
38. Lau CC, Pardee AB. Mechanism by which caffeine potentiates lethality of nitrogen mustard. Proc Natl Acad Sci USA 1982; 79:2942-6.
39. Takagi M, Shigeta T, Asada M, Iwata S, Nakazawa S, Kanke Y, et al. DNA damage-associated cell cycle and cell death control is differentially modulated by caffeine in clones with p53 mutations. Leukemia 1999; 13:70-7.
40. Ormerod MG, Collins MK, Rodriguez-Tarduchy G, Robertson D. Apoptosis in interleukin-3-dependent haemopoietic cells. Quantification by two flow cytometric methods. J Immunol Methods 1992; 153:57-65.
41. Kawatani M, Uchi M, Simizu S, Osada H, Imoto M. Transmembrane domain of Bcl-2 is required for inhibition of ceramide synthesis, but not cytochrome *c* release in the pathway of inostamycin-induced apoptosis. Exp Cell Res 2003; 286:57-66.
42. Kawajiri S, Saiki S, Sato S, Sato F, Hatano T, Eguchi H, Hattori N. PINK1 is recruited to mitochondria with parkin and associates with LC3 in mitophagy. FEBS Lett 2010; 584:1073-9.
43. Sarkar S, Davies JE, Huang Z, Tunnacliffe A, Rubinsztein DC. Trehalose, a novel mTOR-independent autophagy enhancer, accelerates the clearance of mutant huntingtin and alpha-synuclein. J Biol Chem 2007; 282:5641-52.

Neuroscience Letters 481 (2010) 88–91

Contents lists available at ScienceDirect

Neuroscience Letters

journal homepage: www.elsevier.com/locate/neulet

Zonisamide reduces cell death in SH-SY5Y cells via an anti-apoptotic effect and by upregulating MnSOD

Sumihiro Kawajiri[a,1], Yutaka Machida[b,1], Shinji Saiki[a], Shigeto Sato[a], Nobutaka Hattori[a,*]

[a] Department of Neurology, Juntendo University School of Medicine, 2-1-1 Hongo, Bunkyo-ku, Tokyo, 113-8421, Japan
[b] Department of Neurology, Juntendo University Nerima Hospital, 3-1-10 Takanodai, Nerima-ku, Tokyo, 177-0033, Japan

ARTICLE INFO

Article history:
Received 15 April 2010
Received in revised form 8 June 2010
Accepted 21 June 2010

Keywords:
Zonisamide
Apoptosis
Manganese superoxide dismutase
Parkinson's disease

ABSTRACT

Zonisamide, originally known as an antiepileptic drug, has been approved in Japan as adjunctive therapy with levodopa for the treatment of Parkinson's disease (PD). Although zonisamide reduces neurotoxicity, the precise mechanism of this action is not known. Here, we show that zonisamide increases cell viability in SH-SY5Y cells via an anti-apoptotic effect and by upregulating levels of manganese superoxide dismutase (MnSOD). These results would give us novel evidences of PD treatment.

Parkinson's disease (PD) is the second most common neurodegenerative disease characterized by pronounced loss of dopaminergic neurons in the substantia nigra pars compacta. At present, there is no known treatment to suppress the progression of this cell death and the goal of current therapies is only to alleviate symptoms. New therapies are, therefore, required to delay disease progression and to improve the long-term prognosis of PD. Mitochondrial dysfunction due to oxidative stress has been proposed as a major factor in the pathogenesis of PD [3,22] and reduced activity in mitochondrial complex I is associated with PD [13,22]. After complex I blockade with 1-methyl-4-phenyl-1,2,3,6-tetrahydropyridine (MPTP) in mice, there is a time-dependent and region-specific activation of mitochondrial cytochrome c, which activates caspase-9 and -3, resulting in apoptosis [20].

Zonisamide, originally known as an anticonvulsant agent, has been approved in Japan as adjunctive therapy with levodopa for patients with PD [15,16]. The mechanism of zonisamide to improve Parkinsonism has been reported to modify the turnover and synthesis of dopamine (DA) [18,28]. Moreover, it has been recently reported that zonisamide attenuates MPTP-induced and 6-hydroxydopamine (6-OHDA)-induced neurotoxicity and dopaminergic neuron-specific oxidative stress in mice [1,2,29,30]. Although zonisamide is likely to delay the progress of PD, the exact mechanism of its action remains unclear.

In this study, we show that zonisamide increases the viability of differentiated SH-SY5Y cells by inhibiting activation of proapoptotic molecules and upregulating levels of manganese superoxide dismutase (MnSOD), also known as superoxide dismutase-2 (SOD2).

The following antibodies were used in this study: anti-caspase-3 antibody (rabbit), anti-caspase-9 antibody (rabbit), and anti-phospho-SAPK/JNK (Thr183/Tyr185) antibody (rabbit) were obtained from Cell Signaling Technology. Anti-actin antibody (mouse) was from Millipore. Anti-MnSOD antibody (rabbit) was from Upstate.

SH-SY5Y cells were grown in Dulbecco's modified Eagle's medium (DMEM) (Sigma) supplemented with 10% fetal bovine serum (FBS) (Sigma) and 1% penicillin–streptomycin (Invitrogen-GIBCO) at 37 °C and 5% CO_2. To induce cell differentiation, SH-SY5Y cells were incubated in complete medium plus 10 μM *all-trans* retinoic acid (Sigma) for 72 h. For pharmacological studies, zonisamide (Dainippon Sumitomo Pharma Co.), staurosporine (Cell Signaling Technology), 1-methyl-4-phenyl-pyridium ion (MPP^+) (Sigma), and dopamine hydrochloride (Sigma) were added at indicated times and concentrations.

Cell viability was assessed by the WST assay; the ability of mitochondrial activity to reduce 2-(2-methoxy-4-nitrophenyl)-3-(4-nitrophenyl)-5-(2,4-disulfophenyl)-2H-tetrazolium monosodium salt (WST-8) to formazan using the Cell Counting Kit-8 (Dojindo, Kumamoto, Japan), according to the manufacturer's instructions.

TdT-mediated dUTP-biotin nick-end labeling (TUNEL) staining was performed using the *In situ* Cell Death Detection Kit, Fluorescein (Roche) according to the manufacturer's instructions. Cells were then mounted with Vectashield containing DAPI (Vector Lab-

* Corresponding author. Tel.: +81 3 3813 3111; fax: +81 3 5800 0547.
E-mail address: nhattori@juntendo.ac.jp (N. Hattori).
[1] Joint first authors.

0304-3940/$ – see front matter © 2010 Elsevier Ireland Ltd. All rights reserved.
doi:10.1016/j.neulet.2010.06.058

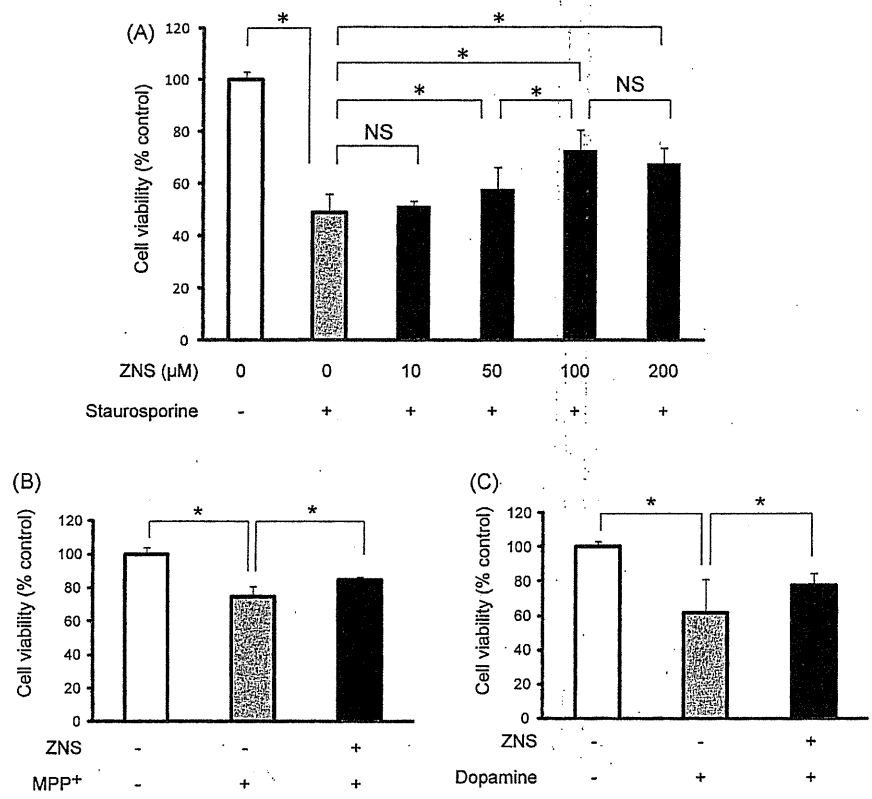

Fig. 1. Zonisamide increases cell viability. (A) Differentiated SH-SY5Y cells were treated with staurosporine (0.2 μM) for 5 h before the WST assay was performed, with or without 24 h treatment with various concentrations of zonisamide. Absorbance at 450 nm was measured. (B) and (C) MPP^+ (500 μM) treatment for 24 h (B), or dopamine (50 μM) treatment for 24 h (C). WST assay was performed with or without 24 h treatment with zonisamide (100 μM). ZNS, zonisamide. *$p < 0.05$. NS, non-significant. Error bars indicate standard deviation of at least five experiments.

oratories, Burlingame, CA, USA) and examined using a fluorescence microscope (BZ-9000; KEYENCE, Japan). Image processing was performed using Adobe Photoshop CS3.

For immunoblot analysis, cells were lysed on ice in lysis buffer [10 mM Tris–HCl (pH 7.5), 150 mM NaCl, 1 mM EDTA, 1% NP-40, and protease inhibitors (complete, Mini, EDTA-free, Roche Applied Science)]. Cell lysates were mixed with NuPAGE 4× LDS sample buffer (Invitrogen). The samples were separated by SDS-PAGE, and proteins were transferred to polyvinylidene fluoride (PVDF) membranes (Millipore). The membranes were blocked with 5% non-fat milk (BD Difco) in Tris-buffered saline containing 0.05% Tween20 (TBS-T) and then incubated overnight at 4 °C with the primary antibody. The membranes were incubated for 1 hour at room temperature with the secondary antibody and visualized using ECL plus reagent (GE Health Care Bio-Sciences) or with Western Lightning (Perkin Elmer-Cetus). After scanning the images, the intensity of each immunoreactive band was estimated by densitometric quantification using ImageJ 1.42 software.

We first examined the effects of zonisamide on the viability of differentiated human neuroblastoma cells (SH-SY5Y cells), which are dopaminergic and can differentiate into neuronal-like phenotypes when treated for 3–5 days with retinoic acid (10 μM). Differentiation is accompanied by the arrest of cell proliferation and increased dopamine metabolism [17,24]. We assessed cell viability using the WST-8 assay [11,25]. In this assay, the tetrazolium salt, WST-8, is cleaved to formazan by a complex cellular mechanism that occurs primarily at the cell surface. This bioreduction is mostly dependent on the production of glycolytic NAD(P)H in viable cells. Therefore, the amount of formazan dye formed directly correlates to the number of metabolically active cells. For staurosporine-treated cells, treatment with zonisamide at 50 μM or over induced an increase of cell viability, with the greatest effect being at 100 μM (Fig. 1A). Subsequent experiments were, therefore, performed using 100 μM zonisamide. Various PD-cellular models have been established using neurotoxins that cause neurotoxicity towards dopaminergic neurons, such as MPTP, DA, rotenone and paraquat [4,5,7,10,23]. Therefore, we next performed similar experiments in the presence of MPP^+ and DA. Zonisamide treatment also prevented subsequence of cell death following MPP^+-treatment (Fig. 1B) and DA-treatment (Fig. 1C). These results indicate that zonisamide has neuroprotective effects in PD-cellular models.

Apoptosis is a major cell death pathway in PD and other neurodegenerative diseases [19]. To investigate the mechanisms by which zonisamide exerts its cytoprotective effects, we examined whether the zonisamide-induced increase of cell viability occurs via an anti-apoptotic effect. We assessed apoptosis in differentiated, staurosporine-treated SH-SY5Y cells using TUNEL staining. As expected, the proportion of TUNEL-positive cells was reduced by zonisamide treatment compared with untreated cells (Fig. 2A and B). To confirm the anti-apoptotic effect of zonisamide, we also examined proapoptotic molecules [caspase-9, -3, and phospho-c-Jun N-terminal kinase (p-JNK)] in differentiated SH-SY5Y cells. Zonisamide treatment reduced the levels of cleaved caspase-9, -3, and p-JNK (Fig. 2C and D). Cleaved caspase-9 is produced in response to mitochondrial damage and the production of cleaved caspase-3 is downstream of cleaved caspase-9. Activation of JNK by reactive oxygen species (ROS) is critical for the induction of apoptosis in neuronal cells [21,27]. Our results suggest that zonisamide blocks the activation of proapoptotic molecules in differentiated SH-SY5Y cells. Also, although PD pathogenesis has been associated with both an excess and a deficiency of autophagic activity [9,26], zonisamide had no effect on autophagic activity because no alteration in the LC3-II/actin ratio, an indicator of autophagic activity, was observed (data not shown).

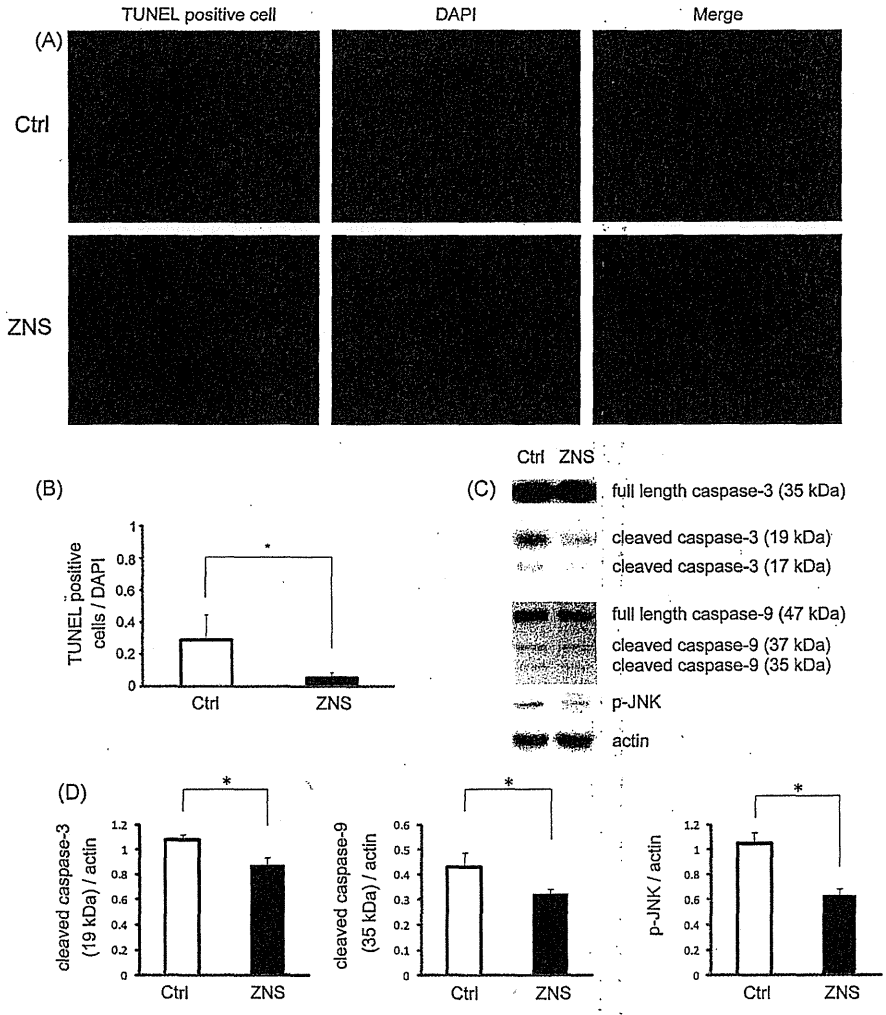

Fig. 2. Zonisamide has anti-apoptotic effects. Differentiated SH-SY5Y cells were treated with staurosporine (0.2 μM) for 3 h, with or without of 24 h treatment with zonisamide (100 μM). (A) TUNEL staining. TUNEL-positive cells are in red. DAPI stained nuclei are in blue. (B) Quantification of TUNEL staining: ratio of TUNEL-positive cells to DAPI stained nuclei is shown. (C) Full length caspase-3, -9, Cleaved caspase-3, -9, and p-JNK levels were analyzed by western blotting. The bottom panel shows actin as a loading control. (D) Quantification of (C): ratios of cleaved caspase-3, -9, and p-JNK to actin are shown. *$p < 0.05$. Error bars indicate standard deviation of at least three independent experiments. Ctrl, control. ZNS, zonisamide.

MnSOD over-expression attenuates MPTP toxicity and protects cells from apoptosis [12,31], while transgenic mice over-expressing MnSOD are more resistant to MPTP toxicity [8]. Based on the results presented in Figs. 1 and 2, we examined whether zonisamide treatment regulates MnSOD activity. We assayed the effects of zonisamide treatment on MnSOD levels in differentiated, staurosporine-treated SH-SY5Y cells. Zonisamide treatment induced an increase in MnSOD levels (Fig. 3A and B). MnSOD is an antioxidant localized in mitochondria and represents a major defense against superoxide free radicals produced in mitochondria. Zonisamide is also known to scavenge hydroxyl radicals and nitric oxide radicals in cell-free systems, which is consistent with our data [2,14]. Although NF-κB is known to be upstream of MnSOD [6], zonisamide treatment did not affect NF-κB levels (data not shown). We did not investigate the zonisamide-induced mechanism of MnSOD upregulation.

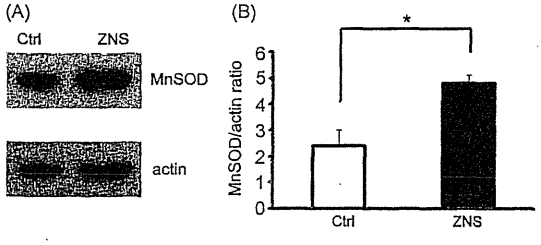

Fig. 3. Zonisamide upregulates levels of MnSOD. (A) Manganese superoxidase dismutase (MnSOD) levels in differentiated SH-SY5Y cells treated with staurosporine (0.2 μM) for 3 h with or without 24 h treatment with zonisamide (100 μM) were analyzed by western blotting. The bottom panel shows actin as a loading control. (B) Quantification of MnSOD western blot: ratio of MnSOD to actin is shown; *$p < 0.05$. Error bars indicate standard deviation of at least three independent experiments. Ctrl, control. ZNS, zonisamide.

In the present study, we provide several lines of evidence showing that zonisamide increased neuronal cell viability via effects on apoptosis and oxidative stress. This interpretation is based on: (1) zonisamide increased cell viability of cells treated with staurosporine and of cells in PD-cellular models. (2) Zonisamide reduced the number of TUNEL-positive cells and the levels of proapoptotic molecules. (3) Zonisamide upregulated levels of MnSOD.

Previous studies have shown that zonisamide significantly attenuates MPTP-induced neurotoxicity by inhibiting microglial activation or 6-OHDA-induced neurotoxicity by increasing glutathione (GSH) via enhancing astroglial cysteine transport system and astroglial proliferation [1,29,30]. However, the direct pharmacological effects on neurons has not been fully investigated. Consistent with previous reports that have investigated cytoprotective effects in PD-cellular models, we demonstrated that

zonisamide inhibited activation of proapoptotic molecules and upregulated levels of MnSOD in neuronal cells without glial cells. Therefore, we assume that zonisamide has direct and indirect effects on neurons, leading to the neuroprotection. Higher levels of MnSOD might be associated with enhanced mitochondrial maintenance and might contribute to reduce apoptosis that has been induced by mitochondrial damage in PD.

In conclusion, our results demonstrate that zonisamide could reduce neuronal cell death via an anti-apoptotic effect and by upregulating MnSOD levels. Although a more detailed elucidation of the action of zonisamide is needed, these results suggest that zonisamide might provide a new approach for the therapy of PD and other progressive neurodegenerative diseases.

Competing financial interest

The authors declare that they have no competing financial interests.

Acknowledgments

We thank Drs. Takeo Arai, Kenya Nishioka and Hattori's laboratory members for helpful discussions. We are grateful to Yoko Imamichi and Akiko Egashira for technical assistance. This study was supported by a Young Scientist Grant (S. Saiki), an All Japan Coffee Association Grant (S. Saiki), a Takeda Scientific Association Grant (S. Saiki) a Grant from Nagao Memorial Fund (S. Saiki) and Health and Labour Science Research Grants for Research on Measures for Intractable Diseases (H15-Intractable-01 and H18-Intracatable-005, N.H.).

References

[1] M. Asanuma, I. Miyazaki, F.J. Diaz-Corrales, N. Kimoto, Y. Kikkawa, M. Takeshima, K. Miyoshi, M. Murata, Neuroprotective effects of zonisamide target astrocyte, Ann. Neurol. 67 (2010) 239–249.
[2] M. Asanuma, I. Miyazaki, F.J. Diaz-Corrales, K. Miyoshi, N. Ogawa, M. Murata, Preventing effects of a novel anti-Parkinsonian agent zonisamide on dopamine quinone formation, Neurosci. Res. 60 (2008) 106–113.
[3] D. Ben-Shachar, P. Riederer, M.B. Youdim, Iron-melanin interaction and lipid peroxidation: implications for Parkinson's disease, J. Neurochem. 57 (1991) 1609–1614.
[4] R.S. Burns, C.C. Chiueh, S.P. Markey, M.H. Ebert, D.M. Jacobowitz, I.J. Kopin, A primate model of Parkinsonism: selective destruction of dopaminergic neurons in the pars compacta of the substantia nigra by N-methyl-4-phenyl-1,2,3,6-tetrahydropyridine, Proc. Natl. Acad. Sci. U.S.A. 80 (1983) 4546–4550.
[5] P.M. Carvey, A. Punati, M.B. Newman, Progressive dopamine neuron loss in Parkinson's disease: the multiple hit hypothesis, Cell Transplant. 15 (2006) 239–250.
[6] M. Djavaheri-Mergny, D. Javelaud, J. Wietzerbin, F. Besancon, NF-kappaB activation prevents apoptotic oxidative stress via an increase of both thioredoxin and MnSOD levels in TNFalpha-treated Ewing sarcoma cells, FEBS Lett. 578 (2004) 111–115.
[7] T.G. Hastings, D.A. Lewis, M.J. Zigmond, Role of oxidation in the neurotoxic effects of intrastriatal dopamine injections, Proc. Natl. Acad. Sci. U.S.A. 93 (1996) 1956–1961.
[8] P. Klivenyi, D. St Clair, M. Wermer, H.C. Yen, T. Oberley, L. Yang, M. Flint Beal, Manganese superoxide dismutase overexpression attenuates MPTP toxicity, Neurobiol. Dis. 5 (1998) 253–258.
[9] M. Komatsu, S. Waguri, T. Chiba, S. Murata, J. Iwata, I. Tanida, T. Ueno, M. Koike, Y. Uchiyama, E. Kominami, K. Tanaka, Loss of autophagy in the central nervous system causes neurodegeneration in mice, Nature 441 (2006) 880–884.
[10] J.W. Langston, I. Irwin, E.B. Langston, L.S. Forno, Pargyline prevents MPTP-induced Parkinsonism in primates, Science 225 (1984) 1480–1482.
[11] Y. Machida, T. Chiba, A. Takayanagi, Y. Tanaka, M. Asanuma, N. Ogawa, A. Koyama, T. Iwatsubo, S. Ito, P.H. Jansen, N. Shimizu, K. Tanaka, Y. Mizuno, N. Hattori, Common anti-apoptotic roles of parkin and alpha-synuclein in human dopaminergic cells, Biochem. Biophys. Res. Commun. 332 (2005) 233–240.
[12] S.K. Manna, H.J. Zhang, T. Yan, L.W. Oberley, B.B. Aggarwal, Overexpression of manganese superoxide dismutase suppresses tumor necrosis factor-induced apoptosis and activation of nuclear transcription factor-kappaB and activated protein-1, J. Biol. Chem. 273 (1998) 13245–13254.
[13] Y. Mizuno, S. Ohta, M. Tanaka, S. Takamiya, K. Suzuki, T. Sato, H. Oya, T. Ozawa, Y. Kagawa, Deficiencies in complex I subunits of the respiratory chain in Parkinson's disease, Biochem. Biophys. Res. Commun. 163 (1989) 1450–1455.
[14] A. Mori, Y. Noda, L. Packer, The anticonvulsant zonisamide scavenges free radicals, Epilepsy Res. 30 (1998) 153–158.
[15] M. Murata, K. Hasegawa, I. Kanazawa, Zonisamide improves motor function in Parkinson disease: a randomized, double-blind study, Neurology 68 (2007) 45–50.
[16] M Murata, E. Horiuchi, I. Kanazawa, Zonisamide has beneficial effects on Parkinson's disease patients, Neurosci. Res. 41 (2001) 397–399.
[17] K. Noda, T. Kitami, W.P. Gai, F. Chegini, P.H. Jensen, T. Fujimura, K. Murayama, K. Tanaka, Y. Mizuno, N. Hattori, Phosphorylated IkappaBalpha is a component of Lewy body of Parkinson's disease, Biochem. Biophys. Res. Commun. 331 (2005) 309–317.
[18] M. Okada, S. Kaneko, T. Hirano, K. Mizuno, T. Kondo, K. Otani, Y. Fukushima, Effects of zonisamide on dopaminergic system, Epilepsy Res. 22 (1995) 193–205.
[19] M. Okouchi, O. Ekshyyan, M. Maracine, T.Y. Aw, Neuronal apoptosis in neurodegeneration, Antioxid. Redox Signal. 9 (2007) 1059–1096.
[20] C. Perier, K. Tieu, C. Guegan, C. Caspersen, V. Jackson-Lewis, V. Carelli, A. Martinuzzi, M. Hirano, S. Przedborski, M. Vila, Complex I deficiency primes Bax-dependent neuronal apoptosis through mitochondrial oxidative damage, Proc. Natl. Acad. Sci. U.S.A. 102 (2005) 19126–19131.
[21] C.G. Pham, S. Papa, C. Bubici, F. Zazzeroni, G. Franzoso, Oxygen JNKies: phosphatases overdose on ROS, Dev. Cell 8 (2005) 452–454.
[22] A.H. Schapira, J.M. Cooper, D. Dexter, P. Jenner, J.B. Clark, C.D. Marsden, Mitochondrial complex I deficiency in Parkinson's disease, Lancet 1 (1989) 1269.
[23] A. Schober, Classic toxin-induced animal models of Parkinson's disease: 6-OHDA and MPTP, Cell Tissue Res. 318 (2004) 215–224.
[24] M. Sharma, P. Sharma, H.C. Pant, CDK-5-mediated neurofilament phosphorylation in SHSY5Y human neuroblastoma cells, J. Neurochem. 73 (1999) 79–86.
[25] M. Shimazawa, Y. Nakajima, Y. Mashima, H. Hara, Docosahexaenoic acid (DHA) has neuroprotective effects against oxidative stress in retinal ganglion cells, Brain Res. 1251 (2009) 269–275.
[26] L. Stefanis, K.E. Larsen, H.J. Rideout, D. Sulzer, L.A. Greene, Expression of A53T mutant but not wild-type alpha-synuclein in PC12 cells induces alterations of the ubiquitin-dependent degradation system, loss of dopamine release, and autophagic cell death, J. Neurosci. 21 (2001) 9549–9560.
[27] Z Xia, M. Dickens, J. Raingeaud, R.J. Davis, M.E. Greenberg, Opposing effects of ERK and JNK-p38 MAP kinases on apoptosis, Science 270 (1995) 1326–1331.
[28] H. Yabe, M.E. Choudhury, M. Kubo, N. Nishikawa, M. Nagai, M. Nomoto, Zonisamide increases dopamine turnover in the striatum of mice and common marmosets treated with MPTP, J. Pharmacol. Sci. 110 (2009) 64–68.
[29] R. Yano, H. Yokoyama, H. Kuroiwa, H. Kato, T. Araki, A novel anti-Parkinsonian agent, zonisamide, attenuates MPTP-induced neurotoxicity in mice, J. Mol. Neurosci. 39 (2009) 211–219.
[30] H Yokoyama, R. Yano, H. Kuroiwa, T. Tsukada, H. Uchida, H. Kato, J. Kasahara, T. Araki, Therapeutic effect of a novel anti-parkinsonian agent zonisamide against MPTP (1-methyl-4-phenyl-1,2,3,6-tetrahydropyridine)neurotoxicity in mice, Metab. Brain Dis. 25 (2010) 135–143.
[31] Y. Zhao, K.K. Kiningham, S.M. Lin, D.K. St Clair, Overexpression of MnSOD protects murine fibrosarcoma cells (FSa-II) from apoptosis and promotes a differentiation program upon treatment with 5-azacytidine: involvement of MAPK and NFkappaB pathways, Antioxid. Redox Signal. 3 (2001) 375–386.

Molecular Brain

RESEARCH Open Access

Distinct mechanisms of axonal globule formation in mice expressing human wild type α-synuclein or dementia with Lewy bodies-linked P123H ß-synuclein

Akio Sekigawa[1], Masayo Fujita[1], Kazunari Sekiyama[1], Yoshiki Takamatsu[1], Taku Hatano[2], Edward Rockenstein[3], Albert R La Spada[4,5], Eliezer Masliah[3] and Makoto Hashimoto[1*]

Abstract

Background: Axonopathy is critical in the early pathogenesis of neurodegenerative diseases, including Parkinson's disease (PD) and dementia with Lewy bodies (DLB). Axonal swellings such as globules and spheroids are a distinct feature of axonopathy and our recent study showed that transgenic (tg) mice expressing DLB-linked P123H β-synuclein (P123H βS) were characterized by P123H βS-immunoreactive axonal swellings (P123H βS-globules). Therefore, the objectives of this study were to evaluate α-synuclein (αS)-immunoreactive axonal swellings (αS-globules) in the brains of tg mice expressing human wild-type αS and to compare them with the globules in P123H βS tg mice.

Results: In αS tg mice, αS-globules were formed in an age-dependent manner in various brain regions, including the thalamus and basal ganglia. These globules were composed of autophagosome-like membranous structures and were reminiscent of P123H βS-globules in P123H βS tg mice. In the αS-globules, frequent clustering and deformation of mitochondria were observed. These changes were associated with oxidative stress, based on staining of nitrated αS and 4-hydroxy-2-nonenal (4-HNE). In accord with the absence of mitochondria in the P123H βS-globules, staining of nitrated αS and 4-HNE in these globules was weaker than that for αS-globules. Leucine-rich repeat kinase 2 (LRRK2), the PARK8 of familial PD, was detected exclusively in αS-globules, suggesting a specific role of this molecule in these globules.

Conclusions: Lysosomal pathology was similarly observed for both αS- and P123H βS-globules, while oxidative stress was associated with the αS-globules, and to a lesser extent with the P123H βS-globules. Other pathologies, such as mitochondrial alteration and LRRK2 accumulation, were exclusively detected for αS-globules. Collectively, both αS- and P123H βS-globules were formed through similar but distinct pathogenic mechanisms. Our findings suggest that synuclein family members might contribute to diverse axonal pathologies.

Keywords: α-synuclein, P123H β-synuclein, Parkinson's disease, Mitochondria, Lysosome, Transgenic mouse

* Correspondence: hashimoto-mk@igakuken.or.jp
[1]Division of Sensory and Motor Systems, Tokyo Metropolitan Institute of Medical Science, Tokyo 156-8506, Japan
Full list of author information is available at the end of the article

Background

α-Synucleinopathies such as Parkinson's disease (PD) and dementia with Lewy bodies (DLB) are leading causes of movement disorders and dementia in aging populations [1,2]. α-Synucleinopathies are characterized by the presence of Lewy bodies and Lewy neurites, which are filled with aggregates of α-synuclein (αS), an abundant nerve terminal protein with unknown functions. It is well established that αS has a central role in the pathogenesis of these diseases, but little is known about the onset and progression of the degenerative process.

Recently, evidence has accumulated to indicate that an axonal pathology caused by αS may play a critical role in the early pathogenesis of α-synucleinopathies. This is supported by the widespread axonal pathology observed from the earliest stages of these disorders, suggesting that axonal function may be impaired in the early pathogenesis [3]. In this context, the appearance of αS-positive Lewy neurites has been shown to precede that of Lewy bodies in brains and cardiac sympathetic neurons. These results suggest that degeneration begins in the distal axon and proceeds towards the cell body in α-synucleinopathies [4,5]. Thus, elucidation of the mechanisms of axonal pathology is important to gain a better understanding of the early pathogenesis of α-synucleinopathies and to establish effective therapeutic agents.

Axonal pathologies such as axonal deposits of αS and axonal swellings have been shown in various lines of transgenic (tg) mice expressing either wild-type αS or βS with PD-linked missense mutations [6-9], but have not been characterized extensively. Furthermore, not only αS, but also two αS-related molecules, β-synuclein (βS) and γ-synuclein (γS), are associated with neuritic pathology [10,11], such as that in dystrophic neurites and spheroid structures, in the brain in synucleinopathies. Thus, it is unclear how the synuclein family of peptides is involved in the axonal pathogenesis. Based on our findings for formation of axonal swellings in tg mice expressing DLB-linked P123H βS [12], we wondered if these swellings might be a useful model to investigate the axonal pathology caused by each synuclein protein. In this context, the objective of the present study was to characterize axonal swellings of tg mice expressing human αS and to compare them with those found in P123HβS tg mice. The results suggest that axonal swellings found in these two types of mice may be formed by similar but distinct mechanisms.

Results

Age-dependent formation of αS-accumulated axonal swellings (αS-globules) in brains of αS tg mice

To evaluate αS-induced axonal pathologies in the brains of αS tg mice, various histological analyses were carried out. Hematoxylin and eosin staining showed no apparent changes (Figure 1a), but immunohistochemistry of brain sections of αS tg mice, but not of their wild type littermates, exhibited formation of strongly αS-immunoreactive axonal swellings in various areas, including the basal ganglia, thalamus, midbrain and olfactory bulb, but not in the cortex and cerebellum (Figure 1, Additional file 1: Figure S1a). These swellings formed in an age-dependent manner, with the highest number occurring in old stage (Figure 1b). The αS-immunoreactive swellings were occasionally immunopositive for heavy chain of kinesin as an axonal marker, but were not stained by eosin or anti-neurofilament-L antibody (Figure 1c), suggesting that they were a type of axonal swellings. In addition, the long-axis diameter of αS-immunoreactive swellings was 6.55 ± 2.56 μm (mean ± S.D., n = 30 globules). Because the diameters of the swellings were less than 20 μm, they were categorized as "globules" (small spheroids). The swellings were not stained by Thioflavin T or Thiazine Red (data not shown) [13,14], suggesting that fibrillation of accumulated αS was not required for formation of αS-globules in brains of αS tg mice.

The αS-globules were immunopositive for several GABAergic markers, including anti-γ-aminobutyric acid (GABA) and anti-glutamic acid decarboxylase (Additional file 2: Figure S2a), and negative for other neuronal markers such as vesicular glutamate transporter-1 or −2, dopamine transporter, vesicular acetylcholine transporter and serotonin (data not shown). These results suggest that the αS-globules might be derived from GABAergic neurons. Furthermore, the αS-globules were highly immunopositive for calbindin D-28 k, but were partially positive for calretinin, and only occasionally positive for parvalbumin (Additional file 2: Figure S2b), suggesting that the globules might be derived from several types of GABAergic neurons. The mechanism through which globules caused by αS are preferentially formed in GABAergic neurons is unclear. However, our results are consistent with previous studies showing that both dopaminergic neurons and other neuronal types, including large cholinergic interneurons and medium-sized GABAergic projection neurons, are involved in the neuritic pathology in the neostriatum of the PD brain.

Lysosomal pathology of αS-globules in brains of αS tg mice

To investigate the ultrastructure of αS-globules in brains of αS tg mice, immunoelectron microscopy was performed (Figure 2). Similarly to the globules in P123H βS tg mice [15], the αS-globules in αS tg mice were characterized by membranous elements including autophagosome-like structures with double membranes (Figure 2a-e), multivesicular bodies (Figure 2b, e) and multilayered membranes (Figure 2d). These results suggest a possible relevance to aberrant regulation of the

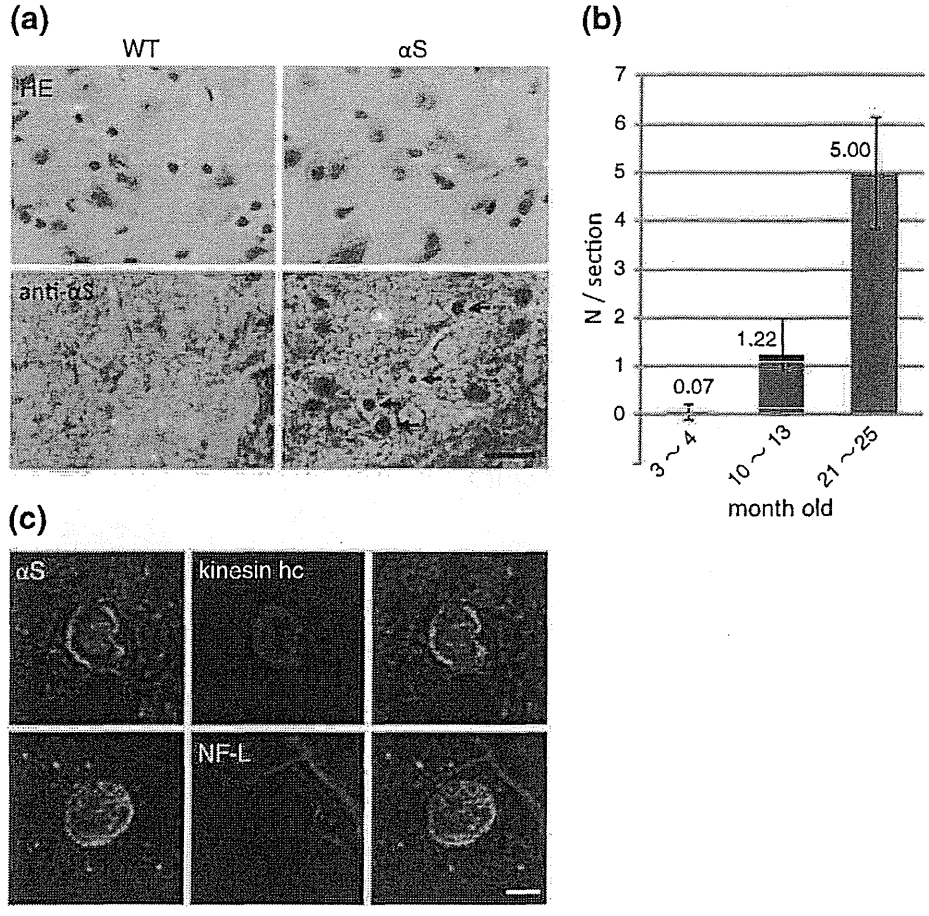

Figure 1 Age-dependent formation of αS-immunopositive axonal swellings (αS-globules) in brains of αS tg mice. (**a**) Hematoxylin and eosin staining (upper two panels) showed no apparent changes in brains of αS tg mice (right) and non-tg littermates (left). Immunohistochemistry of αS (lower two panels) showed formation of αS-globules (arrows) in αS tg mice (right), but not in wild type littermates (left). Representative images for the thalamus are shown. Scale bar = 20 μm. (**b**) Age-dependent formation of αS-globules in the αS tg brain detected by anti-αS antibody. The numbers of globules with diameters >4 μm were unbiasedly counted in the striatum of αS tg brains at three ages: young (n = 5, 3–4 mo), adult (n = 3, 10–13 mo), and old (n = 3, 21–25 mo). (**c**) Double immunofluorescence was performed using αS as a globule identification. Kinesin heavy chain (kinesin hc) was positive (upper three panels) and neurofilament-light (NF-L) was negative (lower three panels). Representative images are shown for the pontine nuclei (upper) and striatum (lower). Scale bar = 5 μm.

autophagy-lysosomal system. Notably, unique membranous structures, comprised of alternating dense and light band forms with a periodicity of 5.8-6.1 nm units and an electron-dense line thickness of 3.3-3.6 nm units, were present in the αS-globules (Figure 2i, j). Moreover, the tubular inclusions (13- to 18-nm diameter) existed in the αS-globules (Figure 2f, h). These structures were reminiscent of the fingerprint profile [16] and curvilinear body [17] that are frequently associated with lysosomal storage diseases such as neuronal ceroid-lipofuscinosis and gangliosidosis. Neither such membranous structures nor Lewy body-like filamentous structures were observed in the somata of αS-expressing neurons.

To characterize the lysosomal pathology in the αS-globules in more detail, an immunofluorescence study was carried out. The globules were immunopositive not only for major gangliosides (GD1a and GM1) but also for some minor gangliosides (GD3, GM2 and GM3) [18,19] (Additional file 3: Figure S3). Based on our previous reports regarding the protective effects of gangliosides on lysosomal pathology in neuroblastoma cells expressing P123H ßS, we speculate that gangliosides might be protective against formation of globules. Finally, the activities of cathepsins B and -D were significantly decreased in αS tg mice compared with non-tg littermates (The mean activity of cathepsin B was 69.8 ± 14.2% and that of cathepsin D was 86.6 ± 10.6%) (Additional file 1: Figure S1, Additional file 4: Additional Methods). These results suggest, but do not prove, that autophagosome-like membranes might accumulate due to decreased clearance by lysosomes. Essentially similar results were previously observed in brains of P123H ßS tg mice [15].

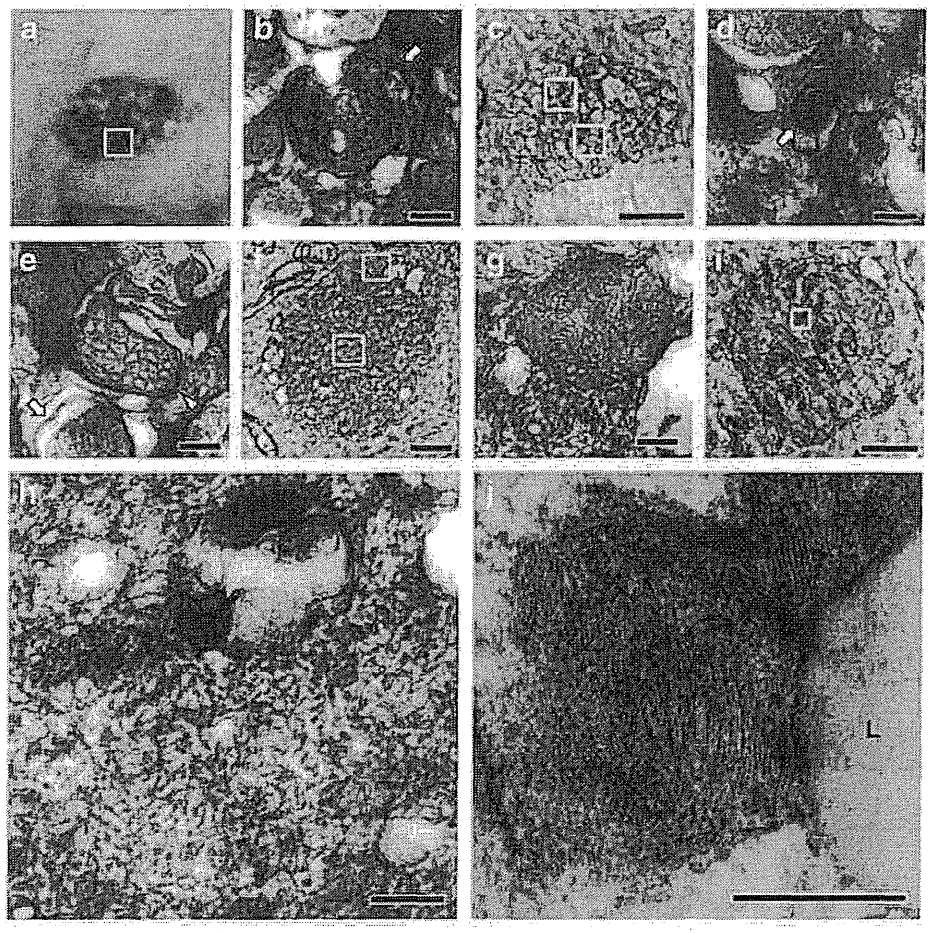

Figure 2 Ultrastructure of αS-globules in brains of αS tg mice. Immunoelectron microscopic analysis was performed using anti-αS. αS-immunopositive globules (**a**) were characterized by lysosomal pathologies such as an αS-immunopositive multivesicular body (**b**: arrow), autophagic vacuoles (**c**), myelinosome (**d**: arrow), a myelinoid membrane (**e**: arrow), and a light multivesicular body (**e**: arrow head). Formation of a fingerprint profile (**j**) adjacent to a lipid droplet (**j**: **L**) and curvilinear bodies (**f**, **h**) are reminiscent of lysosome storage disease. Accumulation of mitochondria was also occasionally observed (**f**, **i**; blue). Some mitochondria were swollen and deformed (**g**). The globules are representatives of those in the thalamus (**a-h**) and striatum (**i**, **j**). The boxed area in panels with lower magnifications (**a**, **c**, **f**, and **i**) were enlarged in **b**, and **j** or in two figures (**d**, **e**, **g**, **h**). Scale bar = 2 μm for **c**, **f**, **i**; 200 nm for **b**, **d**, **e**, **g**, **h**, **j**.

Enhanced oxidative stress with mitochondrial abnormality in αS-globules in brains of αS tg mice

Besides a lysosomal pathology, immunoelectron microscopy showed accumulation of mitochondria in αS-globules in brains of αS tg mice. Some αS-globules displayed clustering of mitochondria (Figure 2f, i), while others had swollen mitochondria in the peripheral regions of the globules (Figure 2g). Consistent with the deformation of the mitochondria, there was a clear decrease in their osmophility (Figure 2g), indicating increased pH in the intermembrane space of mitochondria. However, more severe mitochondrial pathologies, such as distorted and vacuolated mitochondria, were not observed.

To characterize the mitochondrial pathology in the αS-globules, an immunofluorescence study was conducted. The results showed that αS-globules were immunopositive for various mitochondria markers, including voltage-dependent anion channel isoform 1 (VDAC1), cytochrome C and the stress protein heat shock protein 60 (HSP 60) (Figure 3). All VDAC1 immunohistochemical images in αS-globules showed a diffuse pattern (67% in the thalamus, n = 12). This pattern of VDAC1 staining suggested possible damage of mitochondrial outer membrane [20]. However, it is unlikely that apoptosis was involved since cytochrome C and HSP 60 staining was still localized in the swollen mitochondria. The absence of COX IV, a cytochrome C oxidase subunit in the mitochondrial inner membrane, in the αS-globules is consistent with a report showing that genes derived from mitochondrial DNA, including COX IV, are deleted in many cases of sporadic PD [21].

Abnormal accumulation of mitochondria in αS-globules might stimulate oxidative stress. This possibility was assessed based on immunoreactivities to nitrated αS

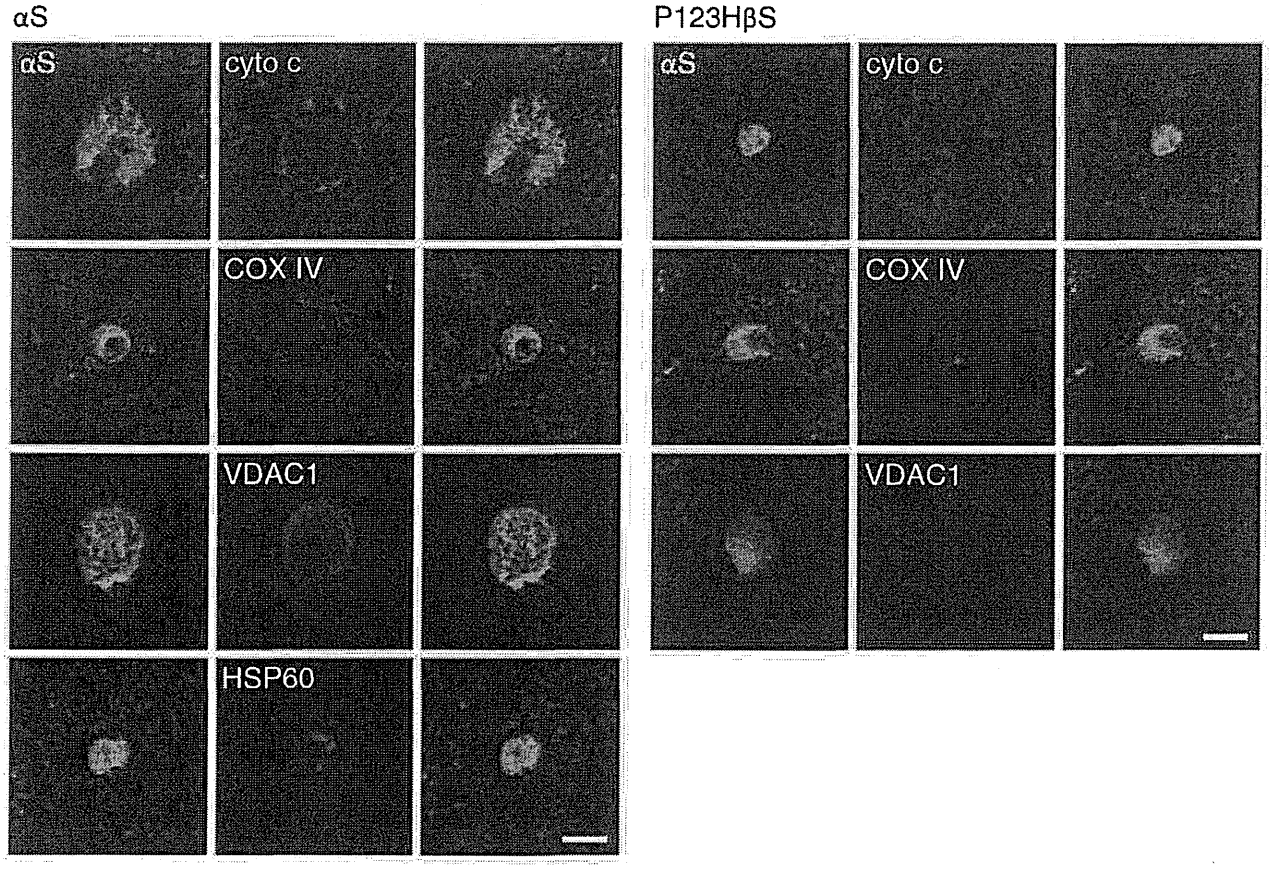

Figure 3 Localization of mitochondrial marker proteins in αS-globules and P123H ßS-globules. Because P123H βS-immunopositive globules in brains of P123H βS tg mice were immunopositive for αS (~100%), double immunofluorescence analyses of αS tg mice (twelve left panels) and P123H ßS tg mice (nine right panels) were performed using αS as a globule identification. In αS tg mice, cytochrome C (upper panels) and HSP60 (lowest panels) showed punctate patterns, while VDAC1 (third panels) was located diffusely. In contrast, COX IV (second panels) was not detected. In P123H βS tg mice, cytochrome C (upper panels), COX IV (middle panels) and VDAC1 (lower panels) were all immunonegative. Representative images are shown for the thalamus in αS tg mice and the basal ganglia in P123H βS tg mice. Scale bar = 5 μm.

and 4-hydroxy-2-nonenal (4-HNE), a product of biological lipid peroxidation (Figure 4) [22,23]. In support of this hypothesis, considerable amounts of the αS-globules were immunostained with anti-nitrated-αS antibody (~61% in the basal ganglia, n = 59), suggesting that nitration was upregulated (Figure 4). Similarly, the αS-globules had the immunoreactivity for anti-4-HNE antibody (~43% in the basal ganglia, n = 54), confirmed that the oxidative stress was increased in the αS-globules (Figure 4). Phosphorylation of αS was evaluated as another possible posttranslational modification, since Lewy bodies in human brains are consistently immunopositive with anti-phospho-αS antibody [22,23]. In αS tg mice, many but not all of the αS-globules were stained with anti-phospho-αS antibody (~62% in the basal ganglia, n = 63), indicating that phosphorylation of αS may not be critical for globule formation.

Oxidative stress without mitochondria in P123H ßS-globules in brains of P123H ßS tg mice

In contrast to the αS-globules, our previous ultrastructural study showed that mitochondria were rarely observed in P123H ßS-globules in brains of P123H ßS tg mice [15]. Similarly to the results in αS tg mice, P123H ßS tg mice had P123H ßS-immunopositive swellings (P123H ßS-globules) derived from GABAergic projection neurons which were immunoreactive for calbindin D-28 k, but were negative for both calretinin and parvalbumin [15]. We observed that the long-axis diameter of P123H ßS-globules (5.70 ± 1.15 μm, mean ± S.D., n = 30 globules) was comparable to that of αS-globules (6.55 ± 2.56 μm. p = 0.10, Student's *t*-test). Staining for VDAC1, cytochrome C and COX IV was negative in P123H ßS-globules in brains of P123H ßS tg mice (Figure 3). In accord with the absence of mitochondria, oxidative stress, as assessed by anti-4HNE antibody, in

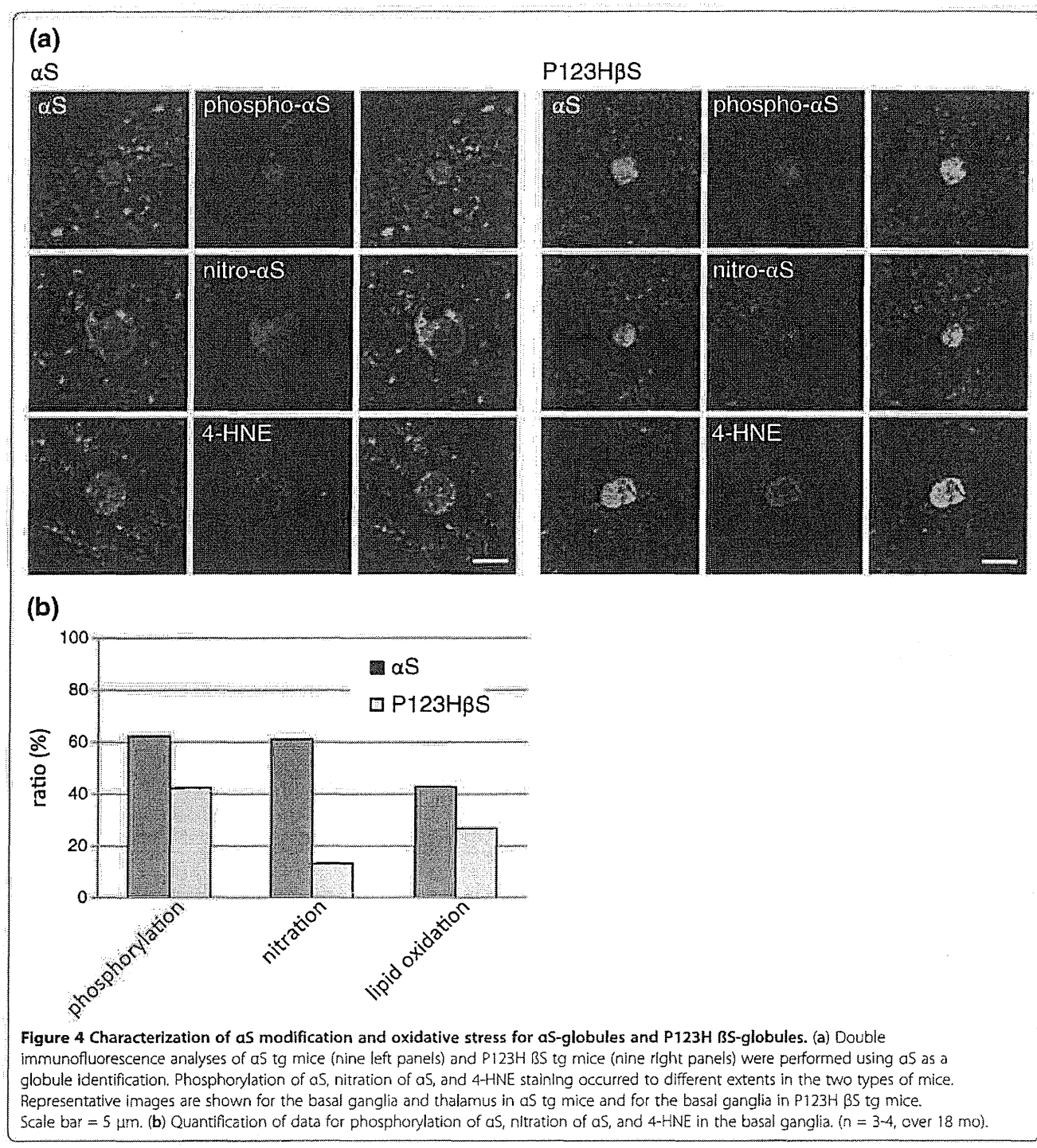

Figure 4 Characterization of αS modification and oxidative stress for αS-globules and P123H ßS-globules. (a) Double immunofluorescence analyses of αS tg mice (nine left panels) and P123H ßS tg mice (nine right panels) were performed using αS as a globule identification. Phosphorylation of αS, nitration of αS, and 4-HNE staining occurred to different extents in the two types of mice. Representative images are shown for the basal ganglia and thalamus in αS tg mice and for the basal ganglia in P123H βS tg mice. Scale bar = 5 μm. (b) Quantification of data for phosphorylation of αS, nitration of αS, and 4-HNE in the basal ganglia. (n = 3-4, over 18 mo).

P123H ßS-globules in P123H ßS tg mice was less than that in αS tg mice (~27% in the basal ganglia, n = 55) (Figure 4). In a similar fashion, nitration of endogenous mouse αS in P123H ßS-globules was negligible (~13% in the basal ganglia, n = 54) (Figure 4), while phosphorylation of endogenous mouse αS in P123H ßS-globules was similar to that in αS-globules in the basal ganglia of αS tg mice (~42% in the basal ganglia, n = 55) (Figure 4).

The mechanism through which P123H βS stimulates formation of globules in the absence of mitochondria in axonal degeneration is unclear. We hypothesized that cholesterol might play a role in the pathogenesis, based on the results of immunoelectron microscopy for P123H

ßS-globules in brains of P123H ßS tg mice, in which approximately half of the globules had accumulation of lipids droplets (Figure 5a). As we expected, cholesterol detection by Schultz staining was highly positive in globules in brains of P123H ßS tg mice (Figure 5b). In contrast, no staining of cholesterol was observed in globules in brains of αS tg mice.

Analysis of familial PD-risk factors in globule formation

Since many familial PD risk factors [24,25] have been implicated in disorders of subcellular organelles such as lysosomes and mitochondria, we examined whether any of these factors were involved in globule formation in αS tg mice or P123H ßS tg mice. Notably, an immunofluorescence study showed frequent detection of leucine-rich repeat kinase 2 (LRRK2) (PARK8) in αS-globules (~79% in the thalamus, n = 28) (Figure 6a). The staining exhibited a small granular dot pattern, suggesting that LRRK2 might be associated with the membranous structures. The specificity of staining was confirmed by preabsorption of the antibody with the immunogen peptides. In contrast, immunoreactivity of LRRK2 was not observed for P123H ßS-globules in the basal ganglia of P123H ßS tg mice (Figure 6b). It is intriguing if absence of LRRK2 in P123H ßS globule might reflect that LRRK2 strictly differentiates human αS from mouse αS and human P123H ßS. Alternative possibility to explain the differential expression of LRRK2 between the αS globule and P123H ßS globule is that LRRK2 might associate with some specific molecules which are expressed only in the αS globule. In this regard, rab5b could be such a candidate since a recent study has well characterized this molecule as a binding partner of LRRK2 [26]. Our immunofluorescence study showed that LRRK2 associates with an endosome molecule Rab5B in axon terminals with a normal range of size, but Rab5B was not detected in the αS-globules (Figure 6c). This result suggests a possibility that LRRK2 have lost the ability to interact with Rab5B, contributing to endosomal deficits during globule formation. Furthermore, although previous reports showed that LRRK2 associated various organelles, such as mitochondria and lysosome [26,27], we did not observed interaction of LRRK2 with mitochondria markers in the αS-globules (data not shown).

Furthermore, despite the accumulation of LRRK2 in the αS-globules, immunoblot analysis [28,29] failed to detect an apparent difference in LRRK2 bands among brain extracts derived from αS tg mice, P123H ßS tg mice, and their wild type littermates (data not shown), possibly due to the relatively small amount of LRRK2 in the αS-globules compared to total LRRK2 in the whole brain.

It has been well characterized that Parkin (PARK2) and PTEN-induced putative kinase 1 (PINK1) (PARK6) are autosomal recessive factors that are critically involved in the maintenance of mitochondrial quality, and that mutations in these genes are causative for mitophagy. However, neither Parkin nor PINK1 was immunopositive in αS- and P123H ßS-globules (Figure 6a). In addition, there was no immunoreactivity for DJ-1 (PARK7) in both types of globules (Figure 6a).

Discussion

Axonal swellings, including globules and spheroids, are characteristic features of axonopathies observed in a number of diseases, including ischemia, trauma, neuroaxonal dystrophy, neurodegenerative disorders, as well as in aging. A recent study suggested that dysfunction of the autophagy-lysosome pathway could be one major contributor to axonal swellings [30,31]. Failure to

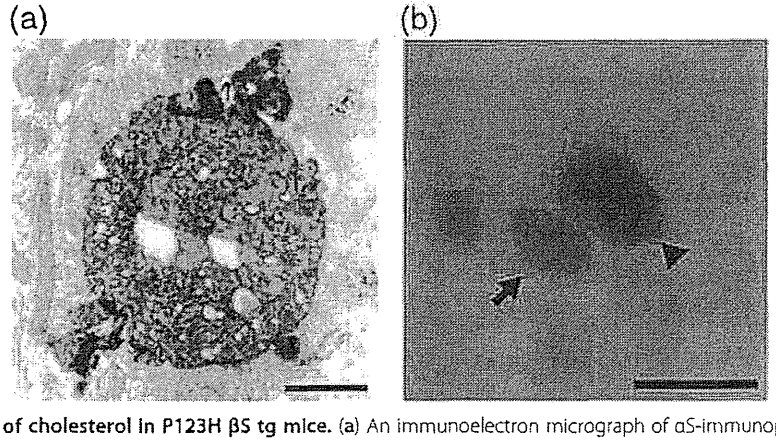

Figure 5 Positive staining of cholesterol in P123H βS tg mice. (**a**) An immunoelectron micrograph of αS-immunopositive globules in the basal ganglia of P123H βS tg mice showed many lipid droplets. Scale bar = 1 μm. (**b**) Detection of cholesterol in the basal ganglia of P123H βS tg mice was performed by Schultz staining. The arrowhead shows cholesterol-positive structure (blue), while the arrow indicates soma containing other lipids (brown). Scale bar = 10 μm.

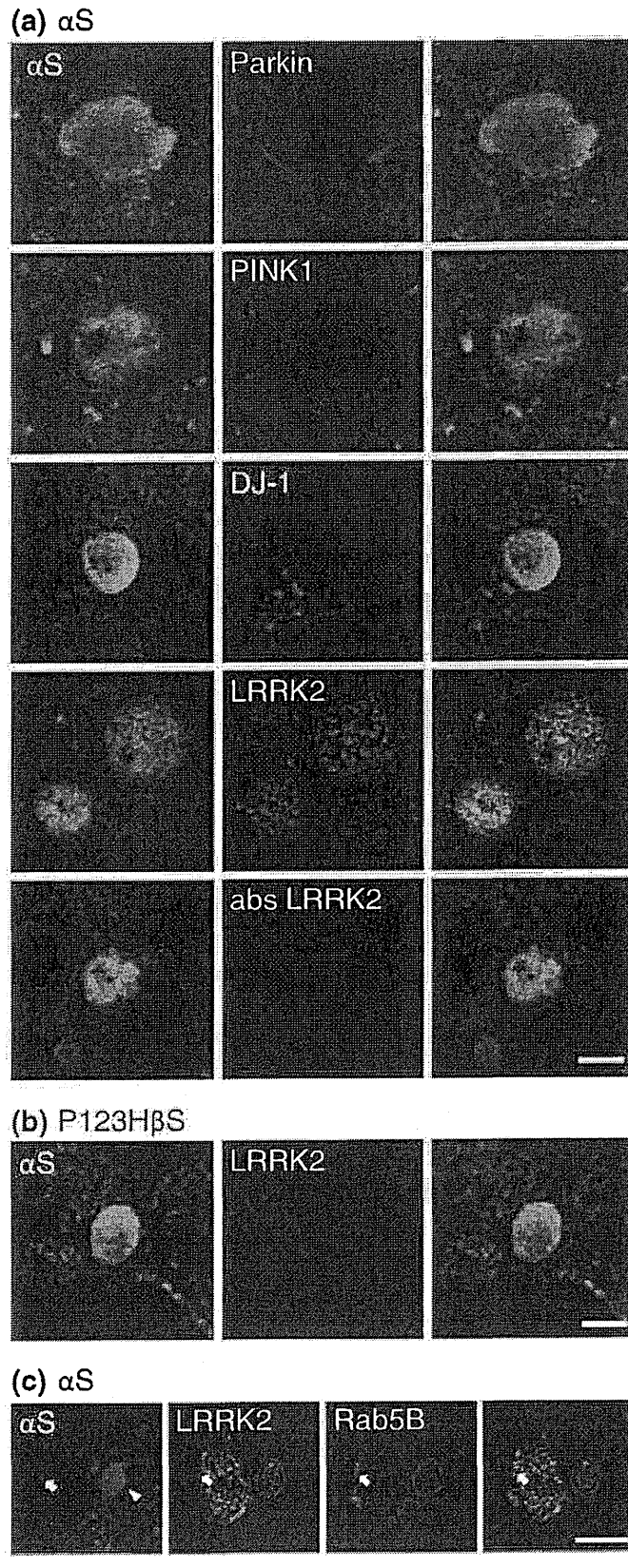

Figure 6 (See legend on next page.)

(See figure on previous page.)
Figure 6 LRRK2 accumulates in globules in αS tg mice. (**a** and **b**) Double immunofluorescence for αS with parkin, PINK1, DJ-1, LRRK2, or negative control (the immunopeptide-preabsorbed anti-LRRK2 antibody) in αS tg mice (**a**) and P123H βS tg mice (**b**). Note that αS-globules were immunopositive for LRRK2 (~79%, n = 22), whereas P123H βS globules were negative for LRRK2. Representative images are shown for the thalamus (αS) and basal ganglia (P123H βS). Scale bar = 5 μm for all panels. (**c**) Triple immunofluorescence for αS, LRRK2 and Rab5B for basal ganglia in αS tg mice. LRRK2 and Rab5B were colocalized in axon terminal (arrow), but were not colocalized in the αS-globule (arrowhead) Scale bar = 10 μm for all panels.

degrade subcellular materials or organelles at distal axons and/or nerve terminals or failure to export these materials by axonal transport has been shown to produce swollen nerve terminals. Such a mechanism might be involved in formation of αS- and P123H βS-globules. In the present study, αS-globules in brains of αS tg mice were characterized by autophagosome-like membranous elements and were immunopositive for various minor gangliosides, which is reminiscent of some types of lysosomal storage disease. Consistent with this, lysosomal activity, as assessed by the activities of cathepsins B and -D, was significantly decreased in brain extracts of αS tg mice compared with those from non-tg littermates. Similar lysosomal dysfunctions were previously observed for P123H βS-globules in brains of P123H βS tg mice. Taken together, these results suggest that downregulation of the lysosome degradation pathway may be a common mechanism leading to globule formation in αS and P123H βS tg mice.

In contrast to the lysosomal pathology, mitochondria accumulated specifically in αS-globules. To the best of our knowledge, only one study has previously described abnormal mitochondria in the axonal pathology in tg mice expressing prion promoter-driven αS [32]. In agreement with this study, immunoelectron microscopy of αS revealed abnormal accumulation of mitochondria in αS-globules. Some αS-globules displayed clustering of mitochondria, while others had swollen mitochondria in the peripheral regions. Immunoreactivities of mitochondrial markers such as VDAC1 and cytochrome C were also found in αS-globules. These results suggest that mitochondria clustering might become hyperactive in response to lysosomal dysfunction. Consistent with these findings, αS-globules were associated with oxidative stress, as assessed by staining of 4-HNE and nitrated αS. Conversely, no evidence of mitochondria was obtained in P123H βS-globules, hence oxidative stress (assessed by 4-HNE staining) was less than that in αS-globules. The mechanism through which P123H βS causes mild level of oxidative stress without mitochondria is unclear, but it is noteworthy that cholesterol staining was positive in P123H βS-globules but not in αS-globules. Given that cholesterol and its metabolites are implicated in oxidative stress in the pathogenesis of neurodegenerative diseases [33], the increased oxidative stress in P123H βS-globules could be partly due to accumulation of cholesterol. A further study is warranted to test this intriguing possibility.

LRRK2 was found to be located in αS-globules and may be actively involved in the axonal pathology. Indeed, it was previously shown that LRRK2 was crucial for regulation of neurite formation and length. Knockdown of LRRK2 led to long, highly branched neuritic processes, whereas constructs with increased kinase activity exhibited short simple processes in neuronal cultures (or transduced nigrostriatal models) [34]. More recently, LRRK2R1441G BAC tg mice were shown to have various characteristic axonal pathologies, including large tyrosine hydroxylase-positive spheroid-like structures, dystrophic neurites and enlarged axonal endings [35]. Although the mechanisms are still unclear, the specific accumulation of LRRK2 in αS-globules naturally leads to the speculation that LRRK2 may cooperate with αS in the axonal pathology. In support of this possibility, both αS and LRRK2 have been shown to be commonly involved in pathologies such as impairment of cytoskeleton dynamics and dysregulation of the protein degradation system. Moreover, it was recently shown that various neuropathological features of A53T αS tg mice, such as impaired microtubule dynamics, Golgi disorganization, and decreased proteasomal activity, were worsened by cross-breeding with LRRK2 tg mice, but ameliorated by genetic ablation of LRRK2 [36]. Further investigation is required to determine whether αS and LRRK2 cooperate with each other to produce diverse pathologies, including axonal degeneration.

Finally, given that P123H βS may represent a rare familial case of DLB, it is important to consider whether wild type βS has any role in the formation of axonal globules in sporadic cases of α-synucleinopathies. In this context, neurite accumulation of βS has been demonstrated in various synucleinopathies, including PD, DLB, and neurodegeneration with brain iron accumulation, type I. Although wild type βS is neuroprotective, this molecule might become pathogenic during aging. It is also possible that wild type βS might become pathogenic under certain extreme conditions or through the action of specific environmental factors, leading to stimulation of globule formation. Thus, it is an intriguing possibility that the synuclein family of peptides might contribute to the formation of diverse axonal pathologies.

Conclusions

The main objectives of this study were to evaluate αS-globules in the brains of tg mice expressing human wild-type αS and to compare them with the P123H βS-globules in P123H βS tg mice. The results showed lysosomal pathology was similarly observed for both αS- and P123H βS-globules. Oxidative stress was associated with the αS-globules, and to a lesser extent with the P123H βS-globules. Other pathologies, such as mitochondrial alteration and LRRK2 accumulation, were exclusively detected for αS-globules. Together, both αS- and P123H βS-globules were formed through similar but distinct pathogenic mechanisms, suggesting that synuclein family members might contribute to diverse axonal pathologies.

Methods

All animal procedures were approved and conducted in accordance with the regulations of the Animal Ethics Review Committee of Tokyo Metropolitan Institute of Medical Sciences. *Thy1*-αS tg mice [37] and *Thy1*-P123H βS tg mice (line C) [15] were analyzed using various histological procedures.

Histology and immunohistochemistry

Tissue preparation

The mice were anesthetized by overdose of pentobarbital and sacrificed by cardiac perfusion using 5 ml of an ice-cold solution of 250 mM sucrose and 5 mM $MgCl_2$ in 0.02 M phosphate buffer (pH 7.4) (PB), followed by treatment with 4% paraformaldehyde, 15% saturated picric acid and 0.05% (for single or double-immunohistochemistry, and histochemistry), 0.5% (for immunoelectron microscopic analysis) or 1% (for GABA immunohistochemistry) glutaraldehyde in 0.1 M PB. Serial sections of 20- or 50-μm thickness were then prepared by a vibrating blade microtome (VT1200S; Leica, Nussloch, Germany). Tissue sections were put in glass tubes containing 15% sucrose in 0.1 M PB for 3 h, in 30% sucrose in 0.1 M PB for 3 h, and kept at −30°C until use [38].

Hematoxylin and eosin staining

Sections were stained with Mayer's haematoxylin and 0.5% eosin. Sections were imaged using a Carl Zeiss (Jena, Germany) microscope.

Antisera

All antisera or monoclonal antibodies were purchased from commercial sources (Table 1).

Immunohistochemistry

The sections were incubated in Tris-buffered saline (TBS) containing 1% sodium borohydrate for 30 min, in addition to treatment with TBS containing 1% H_2O_2 for 30 min in the case of diaminobenzidine staining. They were then incubated with primary antibodies (listed in Table 1) in PBS containing 1% normal horse serum and 0.4% Triton X-100 (except that for the lipids detection) overnight at 4°C, followed by detection with biotinylated secondary antibodies and an avidin-biotin complex kit (Vector Laboratories, Burlingame, CA) [39]. A positive reaction was detected using diaminobenzidine tetrahydrochloride (DAB) containing 0.01% hydrogen peroxide and counterstaining with hematoxylin. For detection with fluorescent dye, the sections were incubated with primary antibodies, followed by Alexa Fluor-conjugated secondary antibodies (Invitrogen, Carlsbad, CA). The sections were observed using a sectioning fluorescence microscopy system (Apotome; Carl Zeiss, Jena, Germany).

Immunoelectron microscopy

The sections were incubated in PB containing 1% sodium borohydrate for 30 min and in TBS containing 1% H_2O_2 for 30 min before incubation with primary antiserum against αS in TBS containing 10% normal goat serum and 2% bovine serum albumin overnight at 4°C. The sections were then incubated in biotin-conjugated secondary antiserum followed by treatment with ABC complex (Vector Laboratories) and staining with nickel-enhanced DAB. The stained sections were postfixed in 1% OsO_4 in 0.1 M PB for 60 min, and then stained with 1% uranyl acetate and dehydrated in graded ethanol. Sections were flat embedded on silicon-coated glass slides in Quetol 812 (Nisshin EM, Tokyo, Japan). Immunopositive tissues were serially sectioned at 70-nm thickness with EM UC7 (Leica), followed by final staining with lead citrate. The labeled αS-globules were photographed using an H-7650 electron microscope (Hitachi, Tokyo, Japan) and image files were made from EM films using a scanner (GT-X970; Epson, Suwa, Japan) [38].

Cholesterol staining

The sections were incubated in 2.5% iron alum solution for 3 days at room temperature. Sections were onto slides, followed by draining the solution and drying. Schultz reagent (mixture of equal parts of glacial acetic acid and concentrated sulfuric acid) was applied onto the slide, and then a glass coverslip was mounted [40]. Sections were imaged using an Olympus (Tokyo, Japan) microscope.

Globule counting

For the caudate and putamen, sagittal sections approximately 1.3-1.9 lateral to the midline were used. The location of the slice and identification of brain regions were determined by comparison to atlas images, as previously described [15]. Fluorescent labeled αS-immunopositive

Table 1 Primary and secondary antisera used in this study

	Antigen	Host	Dilution	Mono/polyclonal	Source
Primary antisera and antibodies					
1	α-synuclein	mouse	1:500 (for EM)	monoclonal	BD Biosciences (610787)
			1:1000 (for GABA FIHC)		
			1:2000		
2	α-synuclein	rabbit	1:50	polyclonal	Cell Signaling (#2628)
3	phosphorylated α-synuclein	mouse	1:2000	monoclonal	WAKO (pSyn#64)
4	nitrated α-synuclein	mouse	1:50	monoclonal	Santa Cruz Biotechnology (sc-32279)
5	4-hydroxy-2-nonenal	mouse	1:40	monoclonal	NOF Corporation (MHN-020P)
6	Calbindin D-28 k	rabbit	1:5000	polyclonal	Swant (CB38)
7	Parvalbumin	mouse	1:2000	monoclonal	Merck Millipore (MAB1572)
8	Calretinin	rabbit	1:2000	polyclonal	Swant (7699/4)
9	Glutamic acid decarboxylase	rabbit	1:2000	polyclonal	BIOMOL (GC3008)
10	GABA	rabbit	1:2000	polyclonal	Sigma (A2052)
11	kinesin, heavy chain	mouse	1:50	monoclonal	Merck Millipore (MAB1614)
12	neurofilament-ilght	mouse	1:200	monoclonal	Sigma (N5139)
13	GD1a	mouse	1:10	monoclonal	Seikagaku Corporation (GMR17)
14	GD3	mouse	1:10	monoclonal	Seikagaku Corporation (GMR19)
15	GM2	mouse	1:10	monoclonal	Seikagaku Corporation (GMB28)
16	GM3	mouse	1:10	monoclonal	Seikagaku Corporation (GMR6)
17	VDAC1	rabbit	1:40	polyclonal	Protein Tech (10866-1-AP)
18	cytochrome c	mouse	1:200	monoclonal	BD Biosciences (556432)
19	COX IV	rabbit	1:100	monoclonal	Cell Signaling (#4850)
20	HSP60	rabbit	1:50	polyclonal	Novus (NB100-91819)
21	Parkin	rabbit	1:100	polyclonal	Merck Millipore (AB9244)
22	PINK1	rabbit	1:50	polyclonal	Novus (NB600-973)
23	DJ-1	rabbit	1:50	polyclonal	abcam (ab74268)
24	LRRK2	rabbit	1:200	polyclonal	Novus (NB300-268)
25	VGAT	guinea pig	1:500	polyclonal	Synaptic Systems (131004)
26	Rab5B	goat	1:50	polyclonal	Santa Cruz Biotechnology (sc-26569)
Fluorescein conjugated probe					
1	Alexa 488 conjugated cholera toxin subunit B		0.5 μg/ml		invitrogen (C-34775)
Fluorescein conjugated secondary antisera					
1	Alexa 488 conjugated anti-mouse IgG	goat	1:200	polyclonal	invitrogen (A-11029)
2	Alexa 488 conjugated anti-rabbit IgG	goat	1:200	polyclonal	invitrogen (A-11034)
3	Alexa 594 conjugated anti-mouse IgG	goat	1:200	polyclonal	invitrogen (A-11032)
4	Alexa 594 conjugated anti-rabbit IgG	goat	1:200	polyclonal	invitrogen (A-11037)
5	Alexa 488 conjugated anti-mouse IgM	goat	1:100	polyclonal	invitrogen (A-21042)
6	Alexa 680 conjugated anti-goat IgG	donkey	1:100	polyclonal	invitrogen (A-21084)
Biotinylated secondary antisera					
1	biotinylated anti-mouse IgG	horse	1:200	polyclonal	Vector (BA-2000)

globules with a long axis ≥4 μm were counted directly under a fluorescent microscope or from photomicrographs of sections.

Statistical analysis

Data are given as the means ± S.D. Statistical analysis was performed using SPSS (SPSS Inc. Chicago, IL). *T*-test was used for confirmation of significant differences among WT or P123HβS tg, and αS tg mice, with $P < 0.05$ considered to indicate a significant difference.

Additional files

Additional file 1: Figure S1. Lysosome and proteasome activities in the brain extracts of αS tg mice. (a) αS-globules were detected in the olfactory bulb (arrow), but not in the cerebellum, of old αS tg mice (24 mo). Scale bar=2 mm (upper panel), 50 μm (lower two panels). (b) Cathepsin B, -D and proteasome activities were measured (Additional file 4: Additional Methods). Activities of lysosome (cathepsins B and –D) were significantly lower ($p<0.05$) in the olfactory bulb but not in the cerebellum in αS tg mice compared to the same areas in non-tg littermates (over 23 mo). In contrast, there were no significant difference in proteasome activities (Peptidyl-glutamyl peptide-hydrolyzing (PGPH) enzyme and chymotrypsin) between αS tg mice and non-tg littermates (mean±S.D.; *$p<0.05$, n=6 per group).

Additional file 2: Figure S2. αS-globules are derived from GABAergic neurons. (a) αS-immunopositive globules in the striatum and thalamus of old αS tg mice (over 18 mo) were consistently immunopositive for GABA and glutamic acid decarboxylase (GAD), and were weakly immunopositive for vesicular GABA transporter (VGAT) (arrowhead). Scale bar=5 μm. (b) Immunoreactivity for calbindin (CB) was consistently observed. Staining was partially positive for parvalbumin (PV) and rarely positive for calretinin (CR) in the thalamus. Scale bar=5 μm.

Additional file 3: Figure S3. Immunoreactivities of gangliosides in αS-globules of αS tg mice. (a) Double immunofluorescence analysis of αS tg mice was performed using αS as a globule identification. αS-immunopositive globules in the thalamus of old αS tg mice (25 mo) were positively stained with various anti-ganglioside antibodies. Scale bar=5 μm. (b) Quantification of these data.

Additional file 4: Additional Methods. Measurement of lysosome and proteasome activity.

Competing Interests

The authors declare no competing financial interests.

Authors' contributions

AS, MF, KS, YT, and ER performed the experiments. AS, TH, ARL, EM and MH designed and analyzed the data. AS, ARL, EM and MH wrote the paper. All authors have read and approved the manuscript.

Acknowledgements

We thank Dr. N. Hattori at the Juntendo University School of Medicine and Drs. H. Kawano, H. Okado, K. Watabe, M. Ichikawa and T. Uchihara at the Tokyo Metropolitan Institute of Medical Science for their continuous encouragements. We also thank staff in Center for Basic Technology Research, Tokyo Metropolitan Institute of Medical Science for the technical assistance. This work was supported in part by a grant-in-aid for Science Research on Innovative Areas ("Brain Environment") from the Ministry of Education, Culture, Sports, Science, and Technology, Japan (to MH), Novartis Foundation for Gerontological Research (to MH) and NIH grants, AG18440, AG022074, AG11385 and NS044233 (to EM).

Author details

[1]Division of Sensory and Motor Systems, Tokyo Metropolitan Institute of Medical Science, Tokyo 156-8506, Japan. [2]Department of Neurology, Juntendo University School of Medicine, 2-1-1 Hongo, Tokyo, Bunkyo 113-8421, Japan. [3]Department of Neurosciences, University of California-San Diego, La Jolla, CA 92093-0624, USA. [4]Department of Pediatrics, and Cellular and Molecular Medicine, University of California-San Diego, La Jolla, CA 92093-0624, USA. [5]Rady Children's Hospital, San Diego, CA 92193, USA.

Received: 11 June 2012 Accepted: 21 September 2012
Published: 26 September 2012

References

1. Trojanowski JQ, Goedert M, Iwatsubo T, Lee VM: **Fatal attractions: abnormal protein aggregation and neuron death in Parkinson's disease and Lewy body dementia.** *Cell Death Differ* 1998, **5**:832–837.
2. Hashimoto M, Masliah E: **Alpha-synuclein in Lewy body disease and Alzheimer's disease.** *Brain Pathol* 1999, **9**:707–720.
3. Braak H, Ghebremedhin E, Rub U, Bratzke H, Del Tredici K: **Stages in the development of Parkinson's disease-related pathology.** *Cell Tissue Res* 2004, **318**:121–134.
4. Braak H, de Vos RA, Bohl J, Del Tredici K: **Gastric alpha-synuclein immunoreactive inclusions in Meissner's and Auerbach's plexuses in cases staged for Parkinson's disease-related brain pathology.** *Neurosci Lett* 2006, **396**:67–72.
5. Orimo S, Uchihara T, Nakamura A, Mori F, Kakita A, Wakabayashi K, Takahashi H: **Axonal alpha-synuclein aggregates herald centripetal degeneration of cardiac sympathetic nerve in Parkinson's disease.** *Brain* 2008, **131**:642–650.
6. Masliah E, Rockenstein E, Veinbergs I, Mallory M, Hashimoto M, Takeda A, Sagara Y, Sisk A, Mucke L: **Dopaminergic loss and inclusion body formation in alpha-synuclein mice: implications for neurodegenerative disorders.** *Science* 2000, **287**:1265–1269.
7. van der Putten H, Wiederhold KH, Probst A, Barbieri S, Mistl C, Danner S, Kauffmann S, Hofele K, Spooren WP, Ruegg MA, *et al*: **Neuropathology in mice expressing human alpha-synuclein.** *The Journal of neuroscience: the official journal of the Society for Neuroscience* 2000, **20**:6021–6029.
8. Giasson BI, Duda JE, Quinn SM, Zhang B, Trojanowski JQ, Lee VM: **Neuronal alpha-synucleinopathy with severe movement disorder in mice expressing A53T human alpha-synuclein.** *Neuron* 2002, **34**:521–533.
9. Lee MK, Stirling W, Xu Y, Xu X, Qui D, Mandir AS, Dawson TM, Copeland NG, Jenkins NA, Price DL: **Human alpha-synuclein-harboring familial Parkinson's disease-linked Ala-53 –> Thr mutation causes neurodegenerative disease with alpha-synuclein aggregation in transgenic mice.** *Proc Natl Acad Sci USA* 2002, **99**:8968–8973.
10. Galvin JE, Uryu K, Lee VM, Trojanowski JQ: **Axon pathology in Parkinson's disease and Lewy body dementia hippocampus contains alpha-, beta-, and gamma-synuclein.** *Proc Natl Acad Sci USA* 1999, **96**:13450–13455.
11. Galvin JE, Giasson B, Hurtig HI, Lee VM, Trojanowski JQ: **Neurodegeneration with brain iron accumulation, type 1 is characterized by alpha-, beta-, and gamma-synuclein neuropathology.** *Am J Pathol* 2000, **157**:361–368.
12. Hashimoto M, La Spada AR: **β-synuclein in the pathogenesis of Parkinson's disease and related α-synucleinopathies: emerging roles and new directions.** *Future Neurology* 2012, **7**:155–163.
13. Sakamoto M, Uchihara T, Hayashi M, Nakamura A, Kikuchi E, Mizutani T, Mizusawa H, Hirai S: **Heterogeneity of nigral and cortical Lewy bodies differentiated by amplified triple-labeling for alpha-synuclein, ubiquitin, and thiazin red.** *Exp Neurol* 2002, **177**:88–94.
14. Kanazawa T, Adachi E, Orimo S, Nakamura A, Mizusawa H, Uchihara T: **Pale neurites, premature alpha-synuclein aggregates with centripetal extension from axon collaterals.** *Brain Pathol* 2012, **22**:67–78.
15. Fujita M, Sugama S, Sekiyama K, Sekigawa A, Tsukui T, Nakai M, Waragai M, Takenouchi T, Takamatsu Y, Wei J, *et al*: **A beta-synuclein mutation linked to dementia produces neurodegeneration when expressed in mouse brain.** *Nat Commun* 2010, **1**:110.
16. Iseki E, Amano N, Yokoi S, Yamada Y, Suzuki K, Yazaki M: **A case of adult neuronal ceroid-lipofuscinosis with the appearance of membranous cytoplasmic bodies localized in the spinal anterior horn.** *Acta Neuropathol* 1987, **72**:362–368.
17. Kurokawa Y, Ueno T, Nakamura N, Kimura N: **Deposits of neuronal ceroid-lipofuscinosis in transitional structures–electron microscopic study.** *Folia Psychiatr Neurol Jpn* 1985, **39**:537–542.

18. Kotani M, Kawashima I, Ozawa H, Terashima T, Tai T: **Differential distribution of major gangliosides in rat central nervous system detected by specific monoclonal antibodies.** *Glycobiology* 1993, **3**:137–146.
19. Kotani M, Kawashima I, Ozawa H, Ogura K, Ishizuka I, Terashima T, Tai T: **Immunohistochemical localization of minor gangliosides in the rat central nervous system.** *Glycobiology* 1994, **4**:855–865.
20. Tomasello F, Messina A, Lartigue L, Schembri L, Medina C, Reina S, Thoraval D, Crouzet M, Ichas F, De Pinto V, De Giorgi F: **Outer membrane VDAC1 controls permeability transition of the inner mitochondrial membrane in cellulo during stress-induced apoptosis.** *Cell Res* 2009, **19**:1363–1376.
21. Bender A, Krishnan KJ, Morris CM, Taylor GA, Reeve AK, Perry RH, Jaros E, Hersheson JS, Betts J, Klopstock T, *et al*: **High levels of mitochondrial DNA deletions in substantia nigra neurons in aging and Parkinson disease.** *Nat Genet* 2006, **38**:515–517.
22. Hayashi Y, Yoshida M, Yamato M, Ide T, Wu Z, Ochi-Shindou M, Kanki T, Kang D, Sunagawa K, Tsutsui H, Nakanishi H: **Reverse of age-dependent memory impairment and mitochondrial DNA damage in microglia by an overexpression of human mitochondrial transcription factor a in mice.** *The Journal of neuroscience: the official journal of the Society for Neuroscience* 2008, **28**:8624–8634.
23. Ubhi K, Lee PH, Adame A, Inglis C, Mante M, Rockenstein E, Stefanova N, Wenning GK, Masliah E: **Mitochondrial inhibitor 3-nitroproprionic acid enhances oxidative modification of alpha-synuclein in a transgenic mouse model of multiple system atrophy.** *J Neurosci Res* 2009, **87**:2728–2739.
24. Belin AC, Westerlund M: **Parkinson's disease: a genetic perspective.** *FEBS J* 2008, **275**:1377–1383.
25. Satake W, Nakabayashi Y, Mizuta I, Hirota Y, Ito C, Kubo M, Kawaguchi T, Tsunoda T, Watanabe M, Takeda A, *et al*: **Genome-wide association study identifies common variants at four loci as genetic risk factors for Parkinson's disease.** *Nat Genet* 2009, **41**:1303–1307.
26. Shin N, Jeong H, Kwon J, Heo HY, Kwon JJ, Yun HJ, Kim CH, Han BS, Tong Y, Shen J, *et al*: **LRRK2 regulates synaptic vesicle endocytosis.** *Exp Cell Res* 2008, **314**:2055–2065.
27. Biskup S, Moore DJ, Celsi F, Higashi S, West AB, Andrabi SA, Kurkinen K, Yu SW, Savitt JM, Waldvogel HJ, *et al*: **Localization of LRRK2 to membranous and vesicular structures in mammalian brain.** *Ann Neurol* 2006, **60**:557–569.
28. Giasson BI, Covy JP, Bonini NM, Hurtig HI, Farrer MJ, Trojanowski JQ, Van Deerlin VM: **Biochemical and pathological characterization of Lrrk2.** *Ann Neurol* 2006, **59**:315–322.
29. Melrose HL, Kent CB, Taylor JP, Dachsel JC, Hinkle KM, Lincoln SJ, Mok SS, Culvenor JG, Masters CL, Tyndall GM, *et al*: **A comparative analysis of leucine-rich repeat kinase 2 (Lrrk2) expression in mouse brain and Lewy body disease.** *Neuroscience* 2007, **147**:1047–1058.
30. Yang DS, Lee JH, Nixon RA: **Monitoring autophagy in Alzheimer's disease and related neurodegenerative diseases.** *Methods Enzymol* 2009, **453**:111–144.
31. Kragh CL, Ubhi K, Wyss-Corey T, Masliah E: **Autophagy in dementias.** *Brain Pathol* 2012, **22**:99–109.
32. Martin LJ, Pan Y, Price AC, Sterling W, Copeland NG, Jenkins NA, Price DL, Lee MK: **Parkinson's disease alpha-synuclein transgenic mice develop neuronal mitochondrial degeneration and cell death.** *The Journal of neuroscience: the official journal of the Society for Neuroscience* 2006, **26**:41–50.
33. Bosco DA, Fowler DM, Zhang Q, Nieva J, Powers ET, Wentworth P Jr, Lerner RA, Kelly JW: **Elevated levels of oxidized cholesterol metabolites in Lewy body disease brains accelerate alpha-synuclein fibrilization.** *Nat Chem Biol* 2006, **2**:249–253.
34. MacLeod D, Dowman J, Hammond R, Leete T, Inoue K, Abeliovich A: **The familial Parkinsonism gene LRRK2 regulates neurite process morphology.** *Neuron* 2006, **52**:587–593.
35. Li Y, Liu W, Oo TF, Wang L, Tang Y, Jackson-Lewis V, Zhou C, Geghman K, Bogdanov M, Przedborski S, *et al*: **Mutant LRRK2(R1441G) BAC transgenic mice recapitulate cardinal features of Parkinson's disease.** *Nat Neurosci* 2009, **12**:826–828.
36. Lin X, Parisiadou L, Gu XL, Wang L, Shim H, Sun L, Xie C, Long CX, Yang WJ, Ding J, *et al*: **Leucine-rich repeat kinase 2 regulates the progression of neuropathology induced by Parkinson's-disease-related mutant alpha-synuclein.** *Neuron* 2009, **64**:807–827.
37. Rockenstein E, Mallory M, Hashimoto M, Song D, Shults CW, Lang I, Masliah E: **Differential neuropathological alterations in transgenic mice expressing alpha-synuclein from the platelet-derived growth factor and Thy-1 promoters.** *J Neurosci Res* 2002, **68**:568–578.
38. Kubota Y, Hatada SN, Kawaguchi Y: **Important factors for the three-dimensional reconstruction of neuronal structures from serial ultrathin sections.** *Frontiers in Neural Circuits* 2009, **3**:4.
39. Maruyama M, Matsumoto H, Fujiwara K, Kitada C, Hinuma S, Onda H, Fujino M, Inoue K: **Immunocytochemical localization of prolactin-releasing peptide in the rat brain.** *Endocrinology* 1999, **140**:2326–2333.
40. Schultz A: **Eine Methode des mikrochemischen Cholesterinnachweises am Gewebsschnitt.** *Zentralblatt fur Allgemeine pathologie und Pathologische Anatomie* 1924, **35**:314–317.

doi:10.1186/1756-6606-5-34
Cite this article as: Sekigawa *et al.*: Distinct mechanisms of axonal globule formation in mice expressing human wild type α-synuclein or dementia with Lewy bodies-linked P123H ß-synuclein. *Molecular Brain* 2012 5:34.